

# Using an In Silico Liver to Evaluate a Hepatic Enzyme Induction Mechanism

C. Anthony Hunt, *Member, IEEE, EMBS*, and Glen E.P. Ropella

**Abstract**—Will enzyme induction (EI) within different hepatic lobular zones, following initial exposure to a single xenobiotic, be homogeneous or heterogeneous? Wet-lab EI experiments, as formulated, are infeasible. The In Silico Liver (ISL) was designed in part to explore plausible answers to such questions. The ISL is synthetic, physiologically based, fine-grained, and multi-agent. It has been validated against *in situ* drug disposition data. Results from simulation experiments falsified the hypothesis that a uniform distribution of simulated drug passing through an ISL will produce uniform EI. The results *may* have a hepatic counterpart. We discuss methodological considerations regarding multi-level observation and manipulation of livers and this new class of models.

## I. INTRODUCTION

The recently validated In Silico Liver (ISL) is an advanced example of what has been referred to as executable biology [1], [2]. We refer to the method as being synthetic [2]–[5]. The ISL has been designed to facilitate achieving a deeper understanding of the complexities of hepatic drug disposition under normal and disease conditions [3]–[5]. It is a constructive (synthetic), heuristic, discrete, multi-level, multi-agent model intended for refining and testing hypotheses about the interacting mechanisms underlying drug disposition.

Enzyme induction (EI) is a simple example of a pharmacological response. It alters normal hepatic clearance patterns creating dosing, drug-interaction, and potential toxicity issues [6]. Because of interindividual variability, study of the time-course of enzyme induction has proven to be problematic, even though linkage between EI phenomena and changes in disposition can have adverse therapeutic consequences, and so need clarification. Does initial induction occur relatively uniformly within hepatic lobules? It is currently infeasible to answer that question using wet-lab experiments. However, we can use the ISL and exploratory modeling methods [7] to study simulated EI in detail. We hypothesize that the *in silico* consequences of EI may have *in vivo* counterparts. Because periportal drug concentrations are the highest, EI in that region for high clearance drugs may be higher than elsewhere. On the other hand, all drug that makes it into the periveneous region is seen by many fewer hepatocytes. It is plausible that for most drugs, periportal induction could be greater than elsewhere.

For simplicity, we test the hypothesis that the magnitude and time course of localized EI within the ISL is reasonably uniform within ISL lobules, following a uniform dose. For testing, we specified a simple EI mechanism and we implemented a measure of enzyme number and a means of visualizing that measure within the ISL. Computational experiments used a hypothetical compound based on an earlier parameterization [3]. Given the results, we reject the above hypothesis. The pattern of induction within an ISL lobule was heterogeneous within and between an ISLs three zones. The experiments also show that the hypothesized EI mechanism is sensitive to the likelihood of metabolism: counter-intuitively, for the EI mechanism as specified, a higher probability of metabolism decreases enzyme induction.

## II. METHODS

### A. Specification and Use of an In Silico Liver

ISL phenotypic attributes mimic those observed *in situ*. The greater the similarity between measured ISL behaviors and known hepatic attributes, the more useful ISLs will become as expressions of relevant, translationally useful hepatic knowledge. With that and other uses in mind [4], [5], we designed ISLs to exhibit three key capabilities: 1) they use *discrete interactions*; 2) ISL observables enable a clear *physiological mapping* between hepatic and model components; and 3) the ISL must be *transparent* so that simulation details can be observed, measured, and visualized. To avoid confusion hereafter and clearly distinguish *in silico* features from corresponding wet-lab features we use SMALL CAPS hereafter when referring to the former.

We discretize hepatic anatomy. Aspects of structure are mapped to directed graph structures. A typical LOBULE is pictured in Fig. 1A. An ISL is more complicated than typical inductive models. See [3]–[5] for detailed descriptions and a full list of parameters. For convenience, an abridged ISL description follows. A portion of the ISLs three-zone, SINUSOIDAL network is presented in Fig. 1B. Flow paths are represented by interconnected directed graphs. Software objects representing sinusoidal spaces and functions are placed at graph nodes: they are agents called Sinusoidal Segments (SSs). Their design is illustrated in Fig. 1C. Each zone contains at least one node. SSs are placed at each node. Graph structure is specified by the number of nodes in each zone and the numbers of intra- and inter-zone connections. Nodes in the zone directly adjacent to the CENTRAL VEIN (CV) are connected to the CV. A graph edge specifies a zero length “flow path.” No intra-zone connections were allowed in Zone III. Assignments of connections are randomized for each run to simulate intrahepatic variability.

---

Manuscript received April 7, 2008. This work was supported in part by the CDH Research Foundation (of which CAH is a Trustee).

Glen E.P. Ropella is a founder of Tempus Dictum Inc. ([tempusdictum.com](http://tempusdictum.com)); he is also a member and C. Anthony Hunt directs the BioSystems Group, the Dept. of Bioengineering and Therapeutic Sciences, 513 Parnassus Ave., S-926, University of California, San Francisco, CA 94143, USA. Phone: 415-476-2455; Email: [a.hunt@ucsf.edu](mailto:a.hunt@ucsf.edu)

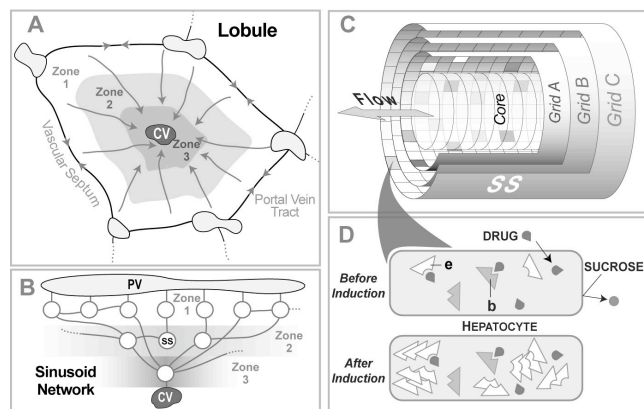


**Fig. 1.** ISL design and components. **A:** A schematic of a cross-section of a hepatic lobule showing the direction of flow from the portal vein tracts (PV), through three zones to the central hepatic vein (CV). **B:** The sinusoid network structure within three lobular zones is represented within the ISL as a 3-zone, interconnected directed graph. Data from the literature were used to constrain graph size and structure. A portion of the graph structure connecting PV outlets to the CV is shown. One SS occupies each graph node. **C:** Objects representing COMPOUNDS (DRUGS) enter and exit via the Core and Grid A, and can access any of the other spaces. Each SS is comprised of three concentric spaces wrapped around a Core. Randomly determined locations within Grids B and C can contain objects representing cells; they are represented using objects called CELLS that function as containers (for other objects). In Grid B CELLS map to endothelial cells and in Grid C they map primarily to hepatocytes. **D:** Shown is a HEPATOCYTE container before and after induction; two types of INTRACELLULAR binders are shown: those that only bind (**b**) and those that also metabolize (**e**); only the latter were used in this study.

### B. SINUSOIDAL SEGMENT Design

Features of lobule heterogeneity are represented by differences within and between SSs. A SS is a tube-like space with a rim surrounded by two spaces. The tube contains a fine-grained abstract “Core” that represents blood. Grid A, the Rim, represents sinusoid edges near endothelial cells. Grid B represents the endothelial layer. Grid C collectively represents the Space of Dissé and hepatocytes. There is no direct coupling between grid locations and real measures such as actual hepatocyte volume or fenestrae size. Resolution is determined by relative grid dimensions and number of SS locations. Grid location properties can be heterogeneous (indicated by the different shadings of Grid A locations in Fig. 1C). Locations not assigned to CELLS in Grid B represent intracellular gaps and fenestrae for object sieving into Grid C; the remainder is assigned to ENDOTHELIAL CELLS. A large fraction of Grid C is assigned to HEPATOCYTES. To reflect the observed relative range of real sinusoid path lengths, each SS length is given by a random draw from a modified gamma distribution having a specified mean and variance (see [3] for details).

### C. Movement of COMPOUNDS within ISL Components

A mobile object represents compound moving through a lobule. Effective flow pressure within each space is governed by the parameter *Turbo*. When *Turbo* = 0, a COMPOUND’S movement is specified by a simple random walk. Increasing *Turbo* biases the walk in the CV direction. Additional COMPOUND behaviors are dictated by axioms that specify relationships between COMPOUND properties, location, and proximity to other objects such as CELLS. A CELL

can disallow entry of a COMPOUND such as SUCROSE because it “sees” an assigned property indicating that partitioning is disallowed. Within a CELL, a COMPOUND becomes subject to intracellular environment axioms.

Each SS outlet is connected randomly to at least one receiving SS or the CV. An object will randomly exit one of the  $n$  outlets. SS exit probability is a function of the number of direct connections to downstream SSs, the inlet areas of each of those SSs, and the “concentration” of other COMPOUNDS just inside those SSs. If CONCENTRATION is high at any part of a SS, flow out of that area increases, resulting from the CONCENTRATION gradient and PRESSURE.

The only needed subcellular functions were binding and metabolism. All cellular components that bind or metabolize a compound are conflated into and represented by BINDING and ENZYME objects placed inside CELLS. ENZYMES are assigned randomly to HEPATOCYTES. A COMPOUND moves within a SS using its own parameter values. When a COMPOUND encounters a CELL within Grid B or C it may partition into the CELL. Once inside, ENZYMES are given the opportunity to bind a COMPOUND and subsequently METABOLIZE it. ENZYMES are programmed to recognize substrates and use that information to adjust the probability of being METABOLIZED.

The DOSE for *one* LOBULE execution uses on the order of 5,000 objects, each representing many molecules. One ISL experiment combines the results from 48 independent executions of the same LOBULE. Several stochastic parameters control the ISL organizational and spatial architecture. Together they provide a unique, individual version of the LOBULE where the relative differences are analogous to those within livers. Differences between executions also capture some of the uncertainty about mechanisms in actual livers, and some of the variability across multiple referent livers.

### D. ENZYME Induction: Mechanism and Parameters

The following is an implementation of one of the frequently encountered plausible EI scenarios. Others are possible and can be explored using analogous implementation strategies. When an ENZYME is executed and there is unbound COMPOUND in the INTRACELLULAR mixture, a pseudo-random number (PRN) is drawn to test for a binding event. Binding events are executed instantaneously. When an ENZYME binds a COMPOUND, a release event is placed on the CELL’S discrete event schedule to occur at a constant number of simulation cycles in the future. When the scheduled release time arrives for an ENZYME-BOUND COMPOUND within a HEPATOCYTE, another PRN is drawn to determine if a METABOLITE or the unchanged COMPOUND will be released.

We implemented an ENZYME INDUCTION mechanism that mimics what is believed to occur most often. ENZYME induction is caused by cumulative signals from ENZYMES to their parent HEPATOCYTE. A binding event causes an ENZYME counter to be incremented. When a counter threshold (*InductionThreshold*) is exceeded, an induction request is sent to the HEPATOCYTE. The value of *InductionThreshold* ranged from ten (low induction) to five (medium) to one (high induction). In the medium induction case, an ENZYME must record five binding events within twenty iterations of

the CELL in order for the ENZYME to request that the CELL create another ENZYME. ENZYMES decrement their induction counter when sufficient time passes between consecutive binding events. This accounts for a recovery time from a stimulated induction state toward a normal state as the COMPOUND concentration drops. For the current project, an ENZYME, once formed, is not destroyed.

At each simulation cycle, the HEPATOCYTE schedules a creation event for each induction request and spreads them out in the future to meet but not exceed a specified induction rate, which is currently 0.9 (ENZYMES/cycle). E.g., for an induction rate of 0.1 and a single induction request, an ENZYME creation event is scheduled 10 cycles from the present. When the induction rate is larger and the HEPATOCYTE is faced with 15 induction requests, it will create 10 ENZYMES in the current cycle and five in the next cycle.

The seven parameters governing the above logic are as follows. 1) *BindersPerCellMin* & *-Max* initialize the number of BINDERS in CELLS and ENZYMES in HEPATOCYTES at the beginning of a Monte Carlo run. 2)  $P_m$  tests against a PRN draw to determine whether a COMPOUND is metabolized when it is released. 3) *EnzymeInductionWindow* determines the recovery time (number of simulation cycles) for induction within a stimulated HEPATOCYTE. 4) *EnzymeInductionThreshold* determines how many binding events are needed to cause an ENZYME to send an induction request to its parent HEPATOCYTE. 5) *EnzymeInductionRate* determines how many ENZYMES per HEPATOCYTE can be produced per simulation cycle. 6)  $P_b$  (solute BINDING probability; 0.5 in all experiments) is tested against a PRN draw to determine whether a COMPOUND proximal to an ENZYME is bound. 7) *SoluteBindingCycles* determines the number of cycles between binding and release events.

#### E. ENZYME Induction: Execution and Examination

Several options and systems aspects were considered for observing the consequences of the above EI mechanism. A coarse grained aspect was derived by first capturing the amount of COMPOUND flowing out of the LOBULE as a fraction of the total dosage for each Monte Carlo run (the LOBULE outflow profile). The cumulative output fraction was then calculated. A fine-grained aspect was derived by first capturing the number of ENZYMES in each sinusoidal segment at each simulation cycle for each Monte-Carlo run. The change (growth) in the number of ENZYMES was calculated for each SS; the change was averaged for an experiment. The results provided an average EI activity for each SS.

Experiments were executed on an eight node OSCAR cluster ([oscar.openclustergroup.org/](http://oscar.openclustergroup.org/)) running RedHat's Fedora 5. The distribution of the runs uses MPICH 1.2.7 ([www-unix.mcs.anl.gov/mpi/mpich1/](http://www-unix.mcs.anl.gov/mpi/mpich1/)). The ISL was compiled using GCC 4.1.1 against the Swarm 2.2.3 Objective-C libraries ([swarm.org/wiki/Main\\_Page](http://swarm.org/wiki/Main_Page)). The initial PRN seed extracted from the machine's clock. Each completed experiment is archived and logged with the date and time using a Makefile target. Examination and processing of data from simulations used a combination of Python (2.4.4) and R (2.4.0) ([www.r-project.org/](http://www.r-project.org/)) scripts.

### III. RESULTS

#### A. Sinusoid Network Structure

COMPOUND parameterizations began with ANTIPYRINE [3] and changed thereafter during exploratory modeling. The Sinusoid Network of each LOBULE is complicated: 47 nodes, 39 edges, and two SS types. That detail is needed to provide sufficient variety of path and residence time options so that the appearance of simulated and referent outflow profiles are similar [4], [5]. Parameters have overlapping influences and the map between the parameters, their values, and the observables is nonlinear. There is one, stochastically determined Sinusoid Network (Fig. 1B) for each run. As the DOSE is metered into SSs in Zone 1, sufficient space is needed into which COMPOUNDS can move. In addition, COMPOUNDS at the leading end of a Zone 1 SS need to get out of the way to make room for incoming COMPOUNDS. The larger the DOSE, the larger the sum of entry spaces needs to be. That area is determined by SS circumference (Grid A width) and number of nodes in Zone 1.

#### B. Experiment Data

Eight experiments ( $E_1 - E_8$ ) measured the impact on outflow profiles and changes in enzyme levels within SSs caused by having high, medium, low, or no EI in combination with a probability of METABOLISM ( $P_m$ ) being 0.1 or 0.25. The parameter pairs [ $P_m$ , EI level] were  $E_1$ : [0.1, none];  $E_3$ : [0.1, low];  $E_5$ : [0.1, medium];  $E_7$ : [0.1, high];  $E_2$ : [0.25, none];  $E_4$ : [0.25, low];  $E_6$ : [0.25, medium]; and  $E_8$ : [0.25, high]. Medium EI ( $EIRate = 0.5$ ) means one ENZYME was created for every two CELL iterations; and an ENZYME must see five binding events ( $EIThreshold = 5$ ) within twenty simulation cycles ( $EIWindow = 20$ ; held constant for all eight experiments) before it requested that the CELL create another ENZYME. The other  $EIRate/EIThreshold$  ratios were 0.1/10 for low and 0.9/1 for high EI. The first DOSE was given five SECONDS after the start of an experiment and the second after 100 SECONDS. The cumulative amount of DRUG collected at the CV was recorded along with the increase in ENZYMES in each SS.

The results without EI (dotted curves in Fig. 2) show essentially the same outflow accumulation for each DOSE; the slightly lower values for  $E_2$  relative to  $E_1$  reflect the higher  $P_m$ . When EI was low ( $E_3$  and  $E_7$ ), there were large, counterintuitive effects. The experiments were repeated and results verified. The explanation traced to the fact that the probability of a COMPOUND being METABOLIZED is conditional: it also depends on BINDING probability ( $P_b = 0.5$  for all eight experiments). By increasing the number of low  $P_m$  ENZYMES for which  $P_b = 0.5$ , we increased the amount of TIME COMPOUNDS were bound and, counter intuitively, decreased the likelihood of METABOLISM. However, when both  $P_m$  and  $P_b$  increased, and ENZYMES numbers also increased (not shown), fraction METABOLIZED increased. Increasing  $P_m$  diminished this counter intuitive effect. For low EI and  $P_m = 0.25$  ( $E_4$ ), the lowered curve (relative to  $E_3$ ) is evidence of increased metabolism. Increasing EI was ini-

tially expected to have a greater impact when  $P_m = 0.25$ , relative to  $P_m = 0.1$ . The data in Fig. 2B show that, because of the conditional effect of  $P_b$ , that was not the case. The amounts of EI when  $P_m = 0.1$  were larger than for  $P_m = 0.25$ , in spite of  $P_m$  being larger. The cumulative outflow profiles were not as informative as initially expected.

The relative amounts of EI within an experiment, from one SS to another, changed dramatically in some cases: both within and between zones: EI was heterogeneous. An illustration of that heterogeneity is provided in Fig. 3 for  $E_7$ .

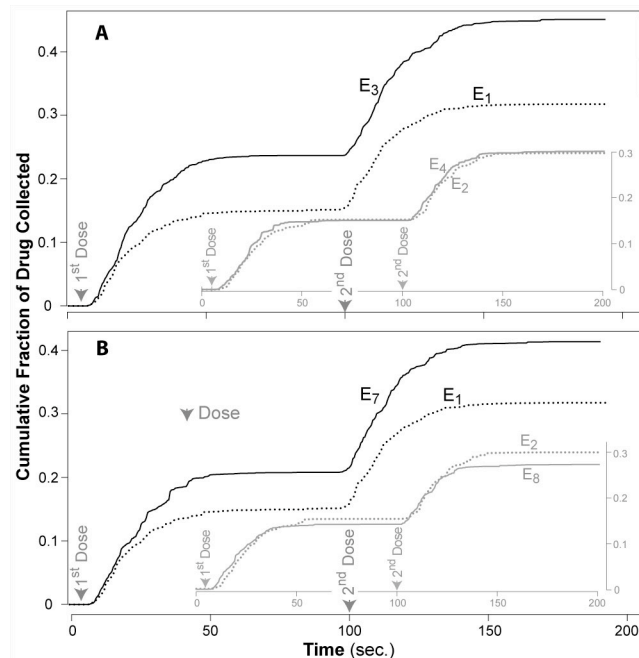


**Fig. 2.** Cumulative outflow profiles (average of 48 Monte Carlo trials). The cumulative fraction (relative to the 1<sup>st</sup> DOSE) of UNMETABOLIZED DRUG, is plotted. Two DOSES were given (arrows). Each DOSE contained equal amounts of SUCROSE and a hypothetical DRUG; only data for the latter are shown. Dotted curves: experiments  $E_1$  and  $E_2$  are controls—no ENZYME INDUCTION; solid curves: experiments  $E_3$  and  $E_4$  had low induction; experiments  $E_7$  and  $E_8$  had high induction.

#### IV. DISCUSSION

The EI distribution in Fig. 3 falsifies our original hypothesis: reasonably uniform EI within ISL LOBULES. There were two interesting results: EI activity across SSs was not uniform, and the magnitude of EI, and thus the relative increase in metabolic clearance, was greater when  $P_m$  was lower. The following is a possible explanation. COMPOUNDS must enter Grid C before EI is even an option. A lower  $P_m$  means more COMPOUNDS survive encounters with ENZYMES, which results in a higher CONCENTRATION of COMPOUND throughout the LOBULE. The implemented EI mechanism is based on ENZYME binding events, which means that EI occurs regardless of whether a COMPOUND is METABOLIZED or not. Hence, a lower  $P_m$  can cause higher EI, more ENZYMES and, counter-intuitively, less extraction, following induction.

The ISL is a large, complicated model with many moving parts. This presents a significant verification problem. We have verified the algorithms inside the ISL on a unit-test and

systemic basis to the extent allowed. Further, the ISL has been validated against in situ data from sucrose and six drugs [4], [5]. Nevertheless, there is ample room within the ISL phenotype to encounter abiotic behavior. Behaviors must be evaluated rigorously and repeatedly. The explanation offered above may be falsified by future experiments. However the very purpose of concept of executable biology and synthetic models of the ISL ilk is to stimulate the formulation of interesting experimental questions to be asked of their referents [1], [2], and these experiments provide an excellent example of such stimulations.

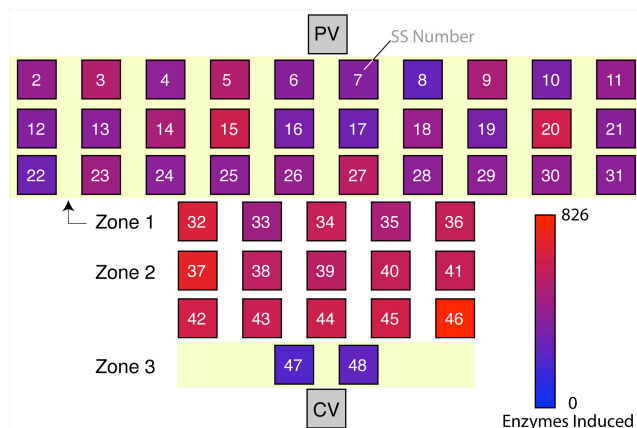


**Fig. 3.** Relative EI between SSs within one study (over 48 Monte Carlo experiments). The 48 SSs are organized by Zone. The fold induction of ENZYMES over the duration of experiment  $E_7$  ( $P_m = 0.1$ ; high EI) from one SS to another, changed dramatically. The greatest induction occurred in Zone 2.

#### ACKNOWLEDGMENT

We thank our collaborator Michael S. Roberts and the members of the BioSystems Group for their comments.

#### REFERENCES

- [1] Fisher J and Henzinger TA (2007) Executable cell biology. *Nat Biotech* 25: 1239-49.
- [2] Hunt CA, Ropella GEP, Park S, and Engelberg J (2008) "Dichotomies Between Computational and Mathematical Models." *Nat Biotech* 26: 737-8.
- [3] Hunt CA, Ropella GEP, Yan, L, Hung DY, and Roberts MS (2006) "Physiologically based synthetic models of hepatic disposition." *J Pharmacokinet Pharmacodyn* 33: 737-72.
- [4] Yan L, Ropella GEP, Park S, Roberts MS, and Hunt CA (2008) Modeling and simulation of hepatic drug disposition using a physiologically based, multi-agent in silico liver. *Pharm Res* 25: 1023-36.
- [5] Yan L, Sheikh-Bahaei S, Park S, Ropella GEP, and Hunt CA (2008) Predictions of hepatic disposition properties using a mechanistically realistic, physiologically based model. *Drug Metab Dispos* 36: 759-68.
- [6] Ropella GEP, Hunt CA, and Nag DA (2005) "Using Heuristic Models to Bridge the Gap between Analytic and Experimental Models in Biology." In L. Yilmaz (ed), *Agent-Directed Simulation Symposium*, Vol. *Simulation Series* 37(2), (ADS'05), SCS Press, San Diego, CA.; pp. 182-90.
- [7] Banks S and Gillogly J (1994) "Exploratory Modeling: Search Through Spaces of Computational Experiments." *Proceedings of the Third Annual Conference on Evolutionary Programming*, Sebald AV, Fogel LJ (eds.), River Edge, New Jersey: World Scientific Publishing Co., pp 353-60.